Rothschild, K. J., Roepe, P., Earnest, T., & Herzfeld, J. (1986) *Proc. Natl. Acad. Sci. U.S.A. 83*, 347-351.
Rothschild, K. J., Bousché, O., Braiman, M. S., Hasselbacher, C. A., & Spudich, J. L. (1988) *Biochemistry 27*, 2420-2424.
Rothschild, K. J., Braiman, M. S., Mogi, T., Stern, L. J., & Khorana, H. G. (1989) *FEBS Lett. 250*, 448-452.
Rothschild, K. J., Braiman, M. S., He, Y. W., Marti, T., & Khorana, H. G. (1990) *J. Biol. Chem. 265*, 16985-16991.
Smith, S. O., Lugtenburg, J., & Mathies, R. A. (1985) *J. Membr. Biol. 85*, 95-109.
Spudich, J. L., & Bogomolni, R. A. (1984) *Nature 312*, 509-513.
Spudich, J. L., & Bogomolni, R. A. (1988) *Annu. Rev. Biophys. Biophys. Chem. 17*, 193-215.
Spudich, J. L., McCain, D. A., Nakanishi, K., Okabe, M., Shimizu, N., Rodman, H., Honig, B., & Bogomolni, R. A. (1986) *Biophys. J. 49*, 479-483.
Spudich, E. N., Takahashi, T., & Spudich, J. L. (1989) *Proc. Natl. Acad. Sci. U.S.A. 86*, 7746-7750.
Stoeckenius, W. (1985) *Trends Biochem. Sci. 10*, 483-486.
Subramaniam, S., Marti, T., & Khorana, H. G. (1990) *Proc. Natl. Acad. Sci. U.S.A. 87*, 1013-1017.
Tittor, J., Soell, C., Oesterhelt, D., Butt, H., & Bamberg, E. (1989) *EMBO J. 8*, 3477-3482.

Population of the Triplet States of Bacteriorhodopsin and of Related Model Compounds by Intramolecular Energy Transfer†

N. Friedman,‡ M. Sheves,*,‡ and M. Ottolenghi*,§
The Weizmann Institute of Science, Rehovot 76100, Israel, and The Hebrew University of Jerusalem, Jerusalem 91904, Israel
Received October 17, 1990; Revised Manuscript Received February 12, 1991

ABSTRACT: In variance with chlorophyll-based photosynthetic pigments, the triplet states of rhodopsins, either visual or photosynthetic, have not been observed experimentally. This is due to the ultrafast crossing from S_1 to S_0, which effectively competes with intersystem crossing to the triplet (T_1) state. In order to populate T_1 indirectly, laser photolysis experiments are performed with model protonated Schiff bases of retinal in solution, in which both inter- and intramolecular energy transfer to the polyene chromophore are carried out from an appropriate triplet energy donor. The experiments are then extended to bacteriorhodopsin (bR) by detaching the native retinal chromophore from the protein-binding site and replacing it by an analogous (synthetic) protonated Schiff base polyene, attached in a nonconjugated way to a naphthone triplet donor. Pulsed laser excitation of the latter moiety led, for the first time, to the observation of the triplet state of a rhodopsin. Possible locations and roles of the T_1 state in bR and in visual pigments are discussed briefly.

Bacteriorhodopsin (bR),[1] the purple membrane pigment in the photosynthetic microorganism *Halobacterium halobium*, as well as visual pigments are both composed of a retinal polyene chromophore bound to the parent protein (opsin) via a protonated Schiff base bound with a lysine residue. It is now well established that in both systems the photocycle is initiated by primary isomerization around a polyene double bond [for reviews see Ottolenghi (1980); Birge (1981, 1989); Packer (1982); Becker (1988); and Ottolenghi and Sheves (1989)]. The subsequent steps initiate the cross-membrane proton pump (in bacteriorhodopsin) or the transduction process (in visual rhodopsins, Rho).

As in the case of chlorophyll-based photosynthetic systems, accumulated evidence suggests that the generation of the primary ground-state photoproducts in the photocycles of bR and Rho, which take place on a subpicosecond time scale, proceeds on an excited singlet potential energy surface with no participation of triplet states. This conclusion is in keeping with the photochemical behavior of model protonated Schiff bases in solution ($RSBH^+$). Thus, although substantial intersystem crossing to the triplet state is observed in the free retinal aldehydes [for a review, see Ottolenghi (1980)], cis ↔ trans isomerization about double bonds is the major detectable photoprocess in $RSBH^+$ (Becker & Freedman, 1985; Becker et al., 1985; Freedman & Becker, 1986). The intersystem crossing yield in $RSBH^+$ is extremely small ($\sim 10^{-4}$) so that triplet-state generation from the singlet manifold can be observed only under the multiple excitation conditions prevailing in high-power laser pulses (Friedman et al., 1989). Apart from the primary photoisomerization, the possible role of the triplet state in visual and photosynthetic rhodopsin has also been discussed in relation to the reverse thermal reaction from primary photoproducts such as bathorhodopsin (in Rho) or K (in bR) back to the parent pigments (Friedman et al., 1989).

In variance with chlorophyll-based photosynthetic pigments, the triplet state of visual or photosynthetic rhodopsins has not been detected experimentally. Our major objective in the present work was to gain direct information on the triplet state of a rhodopsin by populating it selectively via energy transfer. Intermolecular energy transfer has been applied to generate

† This work was supported by the United States-Israel Binational Science Foundation, by the Fund for Basic Research (administered by the Israeli Academy of Sciences and Humanities), by the E. D. Bergman (Hebrew University) Applied Science Foundation, and by the Yeda Fund (Weizmann Institute of Science).
‡ The Weizmann Institute of Science, Rehovot 76100, Israel.
§ The Hebrew University of Jerusalem, Jerusalem 91904, Israel.

[1] Abbreviations: T_1, triplet state; $RSBH^+$, protonated Schiff base; bR, bacteriorhodopsin; Rho, rhodopsin; DIBAH, diisobutylaluminum hydride; $(Bu)_4NF$, tetrabutylammonium fluoride; TCA, trichloroacetic acid; DMAP, dimethylaminopyridine.

0006-2960/91/0430-5400$02.50/0

the triplet states of model $RSBH^+$ in solution (Fisher & Weiss, 1974; Friedman et al., 1989). In preliminary experiments carried out in our laboratory, we have been unsuccessful in achieving the same goal in bR by doping the purple membrane with triplet-energy donors such as anthracene, 1-naphthaldehyde, or 2-acetonaphthone. Such failure is attributed to the inhibited intramembrane mobility of the donor molecule and/or to a poor accessibility of the retinal-binding site in bR. To circumvent such difficulties, we have approached the problem by applying intramolecular energy transfer, where an appropriate donor is covalently bound to the retinal moiety in a nonconjugated way. The method is applied to both $RSBH^+$ and to bR. In the latter case, the approach is based on preparing an artificial pigment in which the original *all-trans*-retinal polyene is replaced by a retinal analogue carrying a nonconjugated triplet-energy donor [for a recent review on artificial rhodopsins, see Ottolenghi and Sheves (1989)]. Our experiments indicate that the triplet states of both $RSBH^+$-like molecules and (artificial) bR may be generated by intramolecular energy transfer.

Experimental Procedures

Materials. Chromophores XI and XII were synthesized as described in Scheme I. The 1,3-dioxolane derivative (I) was readily formed by a Grignard reaction of 2-(2-bromoethyl)-1,3-dioxolane with 2-naphthaldehyde. Acid hydrolysis yielded the tetrahydrofurans i and ii. Treatment of this mixture with (carbomethoxy)methylenetriphenylphosphorane yielded ester III. These reactions were carried out according to Roush et al. (1982).

The trans isomer (III) was isolated by chromatography (ether:hexane 1:1) and treated with 1.2 equivalents of *t*-butyldimethylsilane chloride and 1.2 equivalents of 4-dimethylaminopyridine in methylene chloride overnight at 20 °C. Extraction, followed by purification by chromatography on silica gel (ether:hexane 1:9), afforded ester IV.

The ester group was reduced with 3 equivalents of diisobutylaluminum hydride at −78 °C in hexane for 30 min. The excess of reagent was destroyed with ethyl acetate; the reaction mixture was warmed to room temperature and extracted with water and ether. The crude oil was purified by silica-gel chromatography (ethyl acetate:hexane 1:4) providing alcohol V, which was oxidized with 5 equivalents of manganese dioxide in methylene chloride for 5 h at 20 °C. The reaction mixture was filtered through Celite, followed by solvent evaporation. The crude oil was chromatographed (ethyl acetate:hexane 1:4) to give aldehyde VI.

Aldehyde VI was condensed with 1.5 equivalents of the sodium salt of diethyl-3-methyl-4-phosphonocrotononitrile in THF at 20 °C for 1 h. The reaction mixture was extracted with water and ether, and the residue was chromatographed (ethyl acetate:hexane 1:4) to give nitrile VII. The latter was treated with 1.5 equivalents of diisobutylaluminum hydride in hexane at −78 °C for 30 min. Wet silica and ether were added, and the mixture was stirred for 2 h at 4 °C followed by filtration through celite and solvent evaporation. Silica-gel chromatography (ethyl acetate:hexane 1:4) gave aldehyde VIII.

The condensation reducing hydrolysis sequence was repeated to give aldehyde X. The *t*-butyldimethylsilyl group was removed by treating X with tributylammonium fluoride in THF at 0 °C for 30 min and 2 h at 20 °C. The reaction mixture was extracted with water and ether, and the residue was chromatographed (ethyl acetate:hexane 1:1) to yield XI. The hydroxyl group was oxidized with manganese dioxide in methylene chloride at room temperature for 5 h. The reaction

Scheme I[a]

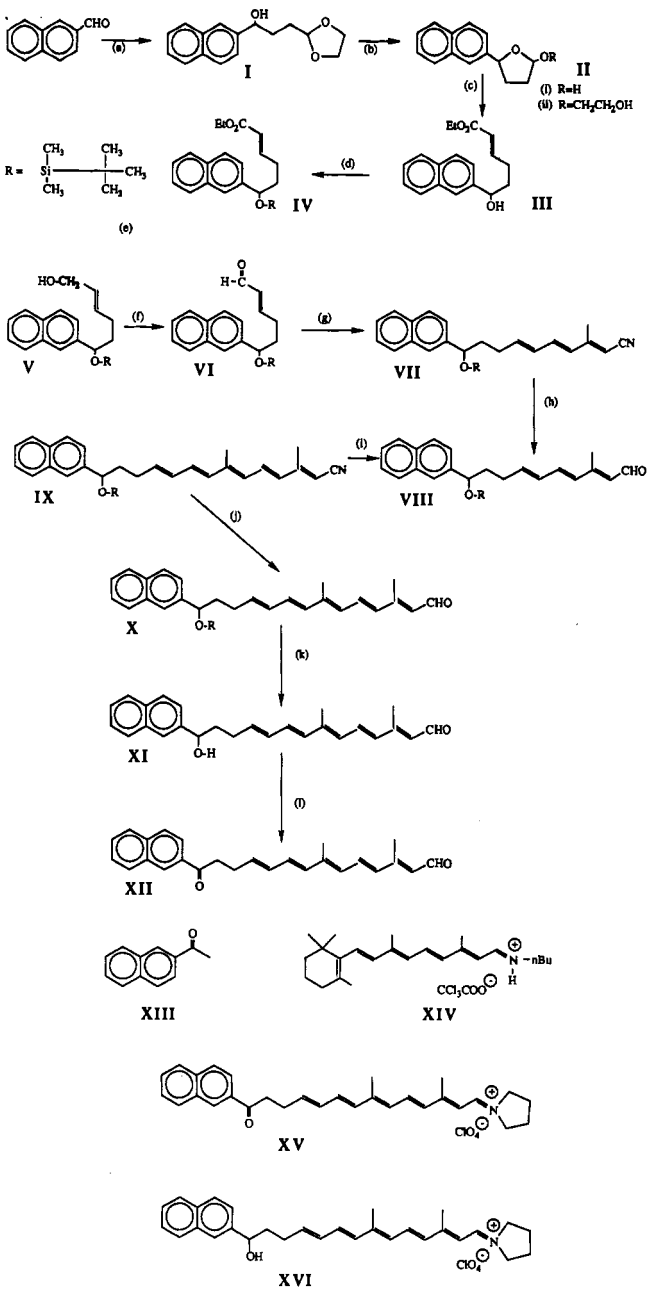

[a] Conditions: (a) $BrCH_2CH_2C(OCH_2)_2$, Mg, THF, 25 °C, 12 h; (b) THF, H_2O, H^+, 25 °C, 24 h; (c) $Ph_3P{=}CHCO_2Et$ CH_2Cl_2, 25 °C, 12 h; (d) 4-DMAP, $(Me)_3C$–$Si(Me)_2$–Cl, CH_2Cl_2, 25 °C, 12 h; (e) DIBAH, *n*-hexane, −78 °C, 30 min; (f) MnO_2, CH_2Cl_2, 25 °C, 5 h; (g) $(EtO)_2P(O)$–$CH_2C(CH_3){=}CHCN$, THF, 25 °C; (h) DIBAH, *n*-hexane, −78 °C, 30 min; (i) $(EtO)_2P(O)$–CH_2–$C(CH_3){=}CHCN$, THF, 25 °C, 1 h; (k) $(Bu)_4NF$, THF, 0 °C for 30 min and 25 °C for 2 h; (l) MnO_2, CH_2Cl_2, 25 °C, 5 h.

mixture was filtered through celite, the solvent was evaporated, and the crude oil was chromatographed (ethyl acetate:hexane 1:4) to give the final product XII, with λ_{max} of 376 nm (EtOH).

Preparation of Protonated Schiff Bases and Pyrrolidinium Perchlorate Salts. The retinal protonated Schiff base ($RSBH^+$) XIV was prepared by mixing the aldehyde with 2.5 equivalents of *n*-$BuNH_2$ in EtOH at 25 °C for 2 h. The solvent and the excess of amine were evaporated, and the residue was dissolved in the proper solvent for measurements. The protonation was carried out by addition of 1 equivalent of trichloroacetic acid. The pyrrolidine perchlorate salts XV and XVI were prepared by mixing chromophores XI and XII

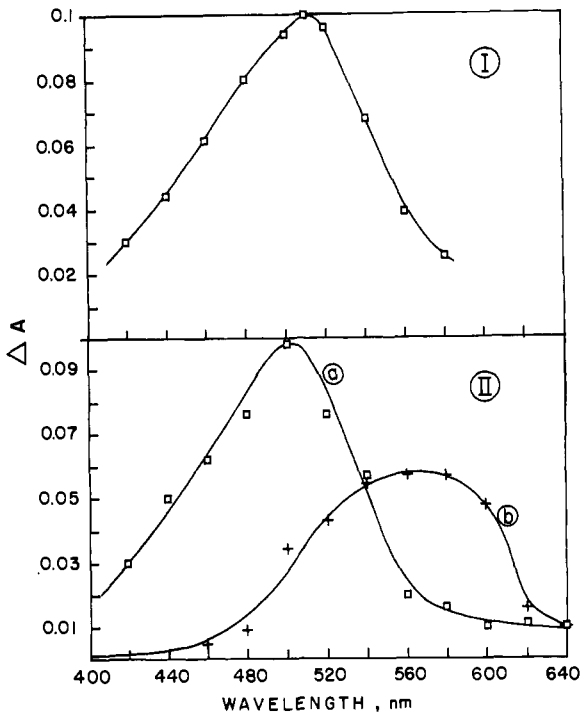

FIGURE 1: (I) Transient absorbance change (ΔD) measured 1 μs after 337.1-nm pulsed laser irradiation of 7.5×10^{-4} M 2-acetonaphthone (XIII) in deaerated ethanol. (II) Same as I in the presence of 1.0×10^{-4} M of $RSBH^+TCA^-$, 1 μs (a) and 10 μs (b) after the pulse.

with pyrrolidine perchlorate in methylene chloride at 25 °C for 1 h.

Artificial Bacteriorhodopsins. Artificial bacteriorhodopsins were prepared by reconstituting the apomembrane with the synthetic retinals. The procedures for apomembrane preparation and reconstitution were those of Tokunaga and Ebrey (1978).

Laser Photolysis. Pulsed-laser photolysis experiments were carried out with a UV-14 DL-200 Molectron N_2/dye laser system (8 ns, 0.2 mJ). Data were digitized with Biomation 8100 or Tektronix 2430 and 7912 transient recorders, followed by computer averaging and analysis.

Results and Discussion

Protonated Schiff Bases in Solution

Intermolecular energy transfer from 2-acetonaphthone (XIII) to a protonated Schiff base of *all-trans*-retinal (XIV, $RSBH^+TCA^-$) is shown in Figure 1. Laser excitation at 337.1 nm of XIII in deaerated ethanol leads to the transient absorption (Figure 1I) of the triplet state of acetonaphthone (λ_{max} = 510 nm, $\tau_{1/2} = 2 \times 10^{-6}$ s). In the presence of a 1.0×10^{-4} M concentration of XIV, the initial absorbance change after the laser pulse, which is identical with that of the acetonaphthone triplet, converts to a transient absorbing around 560 nm (Figure 1II), which decays with a half-life of $\tau_{1/2} = 6.5 \times 10^{-5}$ s. The matching growing-in at 580 nm and decay at 480 nm ($\tau_{1/2} = 5 \times 10^{-7}$ s), along with the effective quenching of the 560-nm species by molecular oxygen, clearly indicate that the latter intermediate should be identified as the triplet state of $RSBH^+$. The results are consistent with pulsed laser experiments in which the same transient species were generated by direct (high-power) excitation of $RSBH^+$ or by energy transfer from the triplet state of anthracene (Friedman et al., 1989). In the present study, the particular choice of the 2-acetonaphthyl moiety as a triplet-energy donor to the polyene was made primarily on the basis of its unity triplet yield, which prevents any substantial contribution of

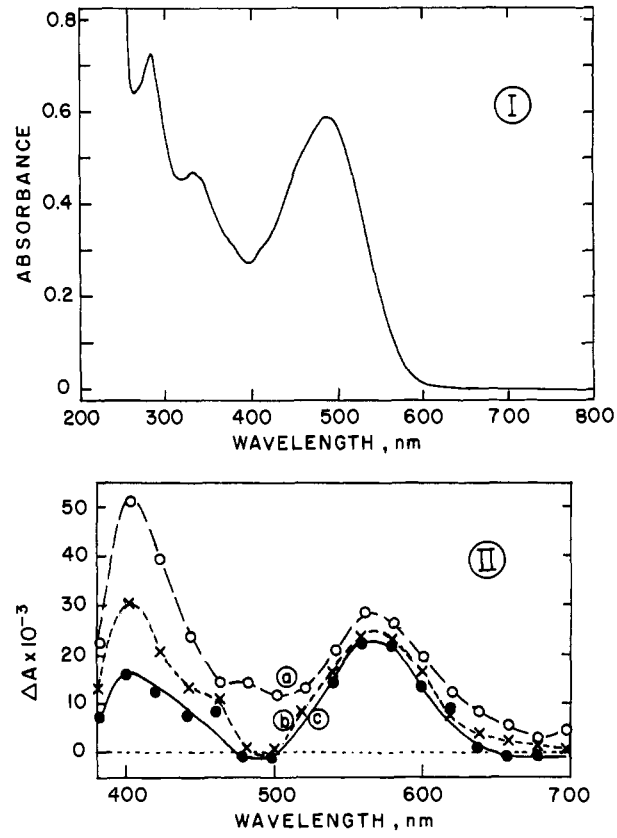

FIGURE 2: (I) Absorption spectrum of the pyrrolidinium perchlorate complex XV (2.0×10^{-4} M) in CH_2Cl_2. (II) Transient photolysis spectra observed after 337.1-nm excitation of XV ($\sim 3.0 \times 10^{-4}$ M in CH_2Cl_2) recorded 0.35 μs (a), 2 μs (b), and 4 μs (c) after the pulse.

singlet (fluorescence) energy transfer. The high triplet energy (E_T = 59 kcal/mol) assures effective energy transfer to the triplet state of the polyene, which lies below the triplet state of anthracene, E_T = 42 kcal/mol (Friedman et al., 1989).

Intramolecular triplet-energy transfer to an analogous retinal polyene system was investigated by laser excitation of the pyrrolidinium perchlorate salt XV. The visible absorption spectrum of the latter (Figure 2I) is close to that of XIV (486 and 475 nm, in methylene chloride, respectively). Pulsed laser (337.1-nm) excitation of XV led to transient absorbance changes that are accounted for by two photoproducts. As shown in Figure 2II, the initial absorbance change consists of a band around 410 nm (shoulder around 480 nm) as well as one around 565 nm. The first exhibits a relatively fast decay ($\tau_{1/2} = 8 \times 10^{-7}$ s^{-1}) that is insensitive to aeration of the solution. The 565-nm species is long-lived ($\tau_{1/2} > 5 \times 10^{-6}$ s) and undergoes quenching by molecular oxygen ($\tau_{1/2} = 3 \times 10^{-5}$ s in aerated solutions).

On the basis of the oxygen sensitivity and the spectroscopic similarity with the triplet state of the protonated Schiff base XIV (consisting of a similar polyene chromophore), we identify the 565-nm intermediate as the triplet state of the bichromophoric compound XV. When considering the data in Figure 2II, it should be noted that absorption of the 337.1-nm laser line is due to both polyene and acetonaphthone chromophores. We assume that these may be approximated as a simple superposition of the spectra of the polyene and of 2-acetonaphthone. From the spectra of protonated Schiff bases and pyrrolidine perchlorate complexes of retinal, we estimate the extinction coefficient of the polyene at 337.1 nm as $\epsilon_{337} \simeq 7000$. Since for the naphthone, $\epsilon_{337} \simeq 2500$, it is evident that 75% of the exciting light is directly absorbed by the polyene. Several arguments lead us to conclude that the 565-nm in-

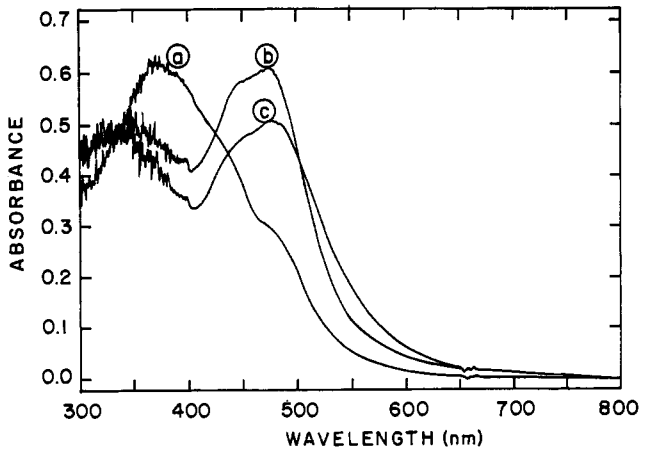

FIGURE 3: Formation of bR(XI) and its light adaptation process. (a) Absorption spectrum 10 s after addition of XI to the bR apomembrane. (b) Absorption spectrum after 30 min of incubation. (c) Absorption spectrum after irradiation of the pigment obtained in (b) at 440 nm.

termediate, identified as the triplet state of XV, is generated by an energy-transfer mechanism, excluding triplet-state generation via intersystem-crossing following direct excitation of the polyene chromophore. First, no 510-nm transient absorbance characteristic of the donor triplet state (Figure 1I) is observed, implying that complete quenching of the latter has occurred over a time scale that is shorter than our time resolution (~50 ns). [In view of the three C–C bond spacing between the donor and acceptor moieties in XV, intramolecular triplet-energy transfer experiments (Closs et al., 1989) predict transfer rates that are of the order of 10^9 s^{-1} or higher]. Second, the 565-nm transient is not observed upon exciting XVI [the hydroxy analogue of XV, where fast singlet (Förster) energy transfer from the aromatic moiety to the polyene is expected to compete effectively with intersystem crossing] or the analogous protonated Schiff base of *all-trans*-retinal (XIV). Since the latter carry polyene chromophores similar to XV, intersystem crossing due to singlet-state excitation of the polyene would be expected to yield the same phototransients for both systems.

At present we are unable to identify the fast decaying, 410-nm, photointermediate of XV. A plausible assignment may involve a single-bond conformer of the polyene system. Control experiments with the analogous chromophore XVI, in which the keto group is replaced by an hydroxy group, shows that the 410-nm ($\tau_{1/2}$ = 10^{-6} s) intermediate is observed in the latter system as well. It should therefore be considered as a photoproduct resulting from direct excitation of the polyene moiety.

Bacteriorhodopsin Pigments

Absorption Spectra. Within 10–30 min after incubation with bacterio-opsin, the characteristic 380–390-nm bands of the free aldehydes, XI and XII, are replaced by a broad visible band centered around 460 nm (see Figure 3). Chromophore competition studies show that when an excess of *all-trans*-retinal is added to the reconstituted systems, the characteristic 575-nm absorption of bR is regenerated within ~12 h. The process is accompanied by disappearance of the 460-nm band. In keeping with this observation, addition of aldehydes XI and XII to unbleached bR does not generate the 460-nm absorption. It is thus suggested that the latter is associated with binding of the synthetic analogues at the retinal-binding site of bR.

The spectra of the artificial pigments derived from analogues XI and XII, denoted as bR(XI) and bR(XII), respectively, are substantially blue-shifted with respect to the 575-nm band

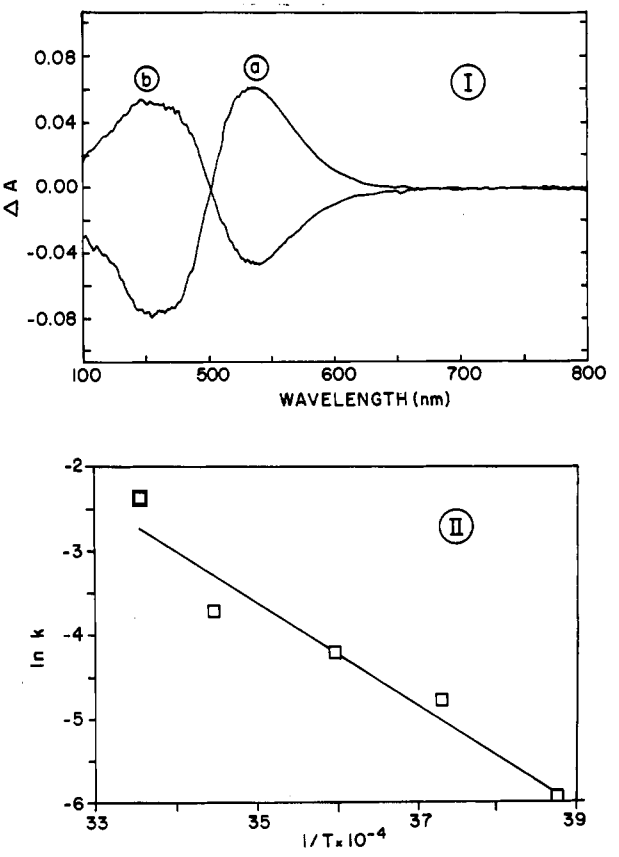

FIGURE 4: Photogeneration and thermal reversibility of the light-adapted modification of bR(XI) and bR(XII). (Ia) Difference spectrum after illumination of bR (XI) with a blue filter (Bb3, 300 nm < λ < 450 nm) at 5 °C. Similar results (not shown) were obtained with bR(XII). (Ib) Difference spectrum following thermal decay of the above solution at 5 °C after 30 min. (II) Arrhenius plot of the dark-adaptation process of pigment bR(XII).

of bR. Both absorption bands are close to those of the corresponding protonated Schiff bases in ethanol solutions (460 nm), implying a negligible "opsin shift" (Nakanishi et al., 1980). (The "opsin shift" is defined as the energy difference between the absorption of the pigment and that of the free protonated Schiff base of the parent chromophore in ethanol.) We have previously shown (Sheves et al., 1984) that bulky substituents at the C_4 retinal ring position of bR induce a comparable shift. The results are interpreted by attributing a substantial fraction of the red spectral shift in native bR to steric ring–chain interactions (a planar conformation) and to electrostatic polyene–protein interactions [for a review, see Ottolenghi and Sheves (1989) and references therein]. Both interactions are removed upon sterically perturbing the ring region of the polyene. The spectra of the present artificial pigments are thus readily accounted for by analogous perturbations, induced by the bulky naphthyl substituents.

Upon exposure of the above artificial pigments to a continuous blue light source, they are partially converted into a red-shifted "light-adapted" modification. As shown in Figure 4I,II, the process is both photoreversible (by illumination with red, λ > 530 nm, light) as well as thermally reversible ($\tau_{1/2}$ = 7.5 s at 20 °C). The decay of the light-adapted species back into the parent pigment is characterized by a first-order rate constant of $k = 5 \times 10^7 \exp(-E_a/RT)$ s^{-1} with E_a = 12.5 ± 1.5 kcal/mol (Figure 4II).

In native bacteriorhodopsin light adaptation is associated with isomerization of a double bond (13-cis → 13-trans) accompanied by a C=N isomerization from syn to anti (Harbison et al., 1984; Smith et al., 1984). It is tempting to suggest

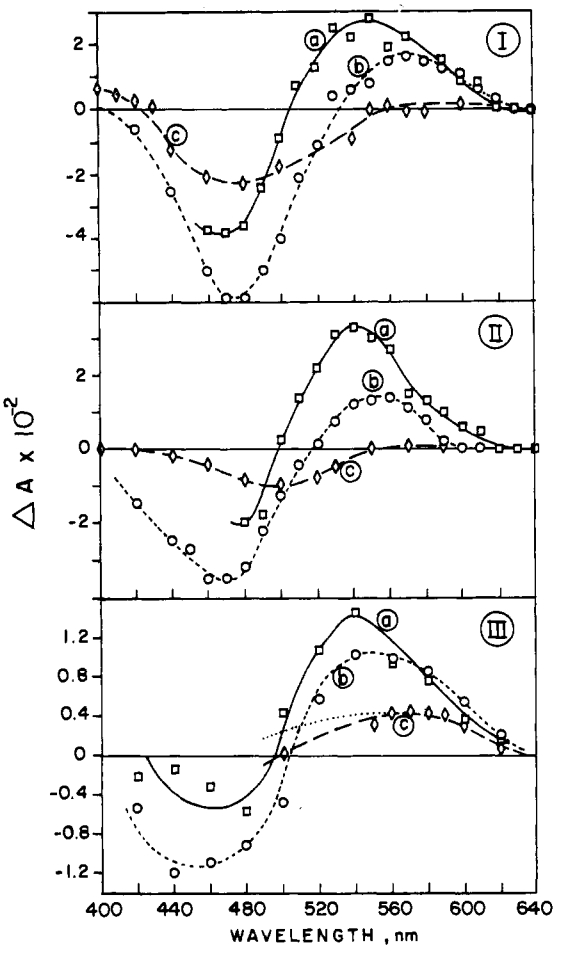

FIGURE 5: The photocycles of bR(XI) and bR(XII). (I) Difference spectra measured after "pulsed" dye laser (496-nm) excitation of bR(XI) 2 μs (a), 40 μs (b), and 4 ms (c) after the pulse. (II) Same as I for the naphthone pigment bR(XII). (III) Difference spectra measured after 337.1-nm excitation of bR(XII). Time values for traces a, b, and c are as in I and II. The dotted line branching from curve IIIc is the net contribution of the triplet difference spectrum. The latter was estimated by correcting for the contribution of the (direct-excitation) photocycle as explained in the text.

that the red-shifted light-adapted modification of the artificial pigments derived from analogues XI and XII is associated as well with simultaneous isomerization of a double bond and of the C=N bond. However, other alternatives, such as single C=N isomerization or a double C=C bond isomerization, are also feasible. The unusual red-shift can be attributed to a modified Schiff base linkage environment leading to weak electrostatic interactions of the positively charged nitrogen with a neighboring negative charge (Baasov et al., 1987). We note that similar phenomena were recently observed with an artificial bacteriorhodopsin pigment derived from 14-*F*-retinal (Tierno et al., 1990).

Pulsed Photolysis Experiments. The dark-adapted forms of the pigments derived from chromophores XI and XII were exposed to pulsed photolysis by dye laser excitation within their visible absorption bands. The light-induced transient spectra are shown in Figure 5. Three distinct stages are clearly evident: (a) an initial rise in the red, denoted here as PK; (b) a subsequent decrease in absorption in the red accompanied by a ~20-nm red-shift, which we denote as PL; and (c) a final, long-lived, stage regenerating the original pigment, which we denote as PM. A comparison between the corresponding photocycle scheme

$$P \xrightarrow{h\nu} PK \xrightarrow{1.5\ \mu s} PL \xrightarrow{500\mu s} PM \xrightarrow{100\ ms} P$$

and that of native bR is not straightforward. Assuming that the dark-adapted form of P is still characterized by an all-trans chromophore, one should look for analogies with the K, L, and M intermediates of the light-adapted (all-trans) bR photocycle. Although the K and PK species resemble both in red-shift (with respect to the parent pigment) and lifetime ($\sim 10^{-6}$ s), PL is markedly red-shifted (while L is not) and exhibits a longer decay time than L. (The absorbance decay time at 560 nm is ~500 μs, as compared with the ~50-μs lifetime of the L → M process in the bR photocycle). Similarly, the PM decay time (100 ms) is longer by almost a factor of 10 than that of M, and, except for a small contribution in the case of the hydroxy pigment, it is not accompanied by an increase in absorbance at 380 nm, characteristic of the deprotonated Schiff base moiety of the M intermediate. Alternatively, if P consists of a 13-cis chromophore, its photocycle should be compared to that of the 13-cis isomer of native bR (Kalisky et al., 1977; Ottolenghi, 1980). The latter consists of a primary, short-lived, red-shifted species, analogous to K and PK, and of a secondary long-lived (~30 ms) red-shifted intermediate, which regenerates the original pigment. Here too, there is no simple exact correlation between the photocycles of the two pigments. It should be pointed out, however, that independently of the isomer composition in P, the primary photoproduct (PK) is analogous with respect to both spectral shift and lifetime to the K species in the photocycles of both 13-*cis*- and *all-trans*-bR.

Experiments were also carried out in deaerated solutions with 337.1-nm excitation. As in the case of XV, the relative contributions of the protonated Schiff base polyene and of the naphthone moiety to the absorbance of bR(XII) at this wavelength were estimated as 75% and 25%, respectively. As shown in Figure 5III for the case of the naphthone pigment, the early difference spectra recorded on a 1–40-μs time scale are reminiscent of those observed following excitation in the visible range (Figure 5II). However, the difference spectra markedly differ at longer times. Thus, in the case of 337.1-nm excitation, a long-lived increase in absorbance ($\tau_{1/2} \simeq 150$ ms) is observed (Figure 5IIIc) that is absent in the visible-excitation photocycle (Figure 5IIc). Repetitive 337.1-nm excitation experiments using the hydroxy pigment, which is inefficient as triplet-energy donor, revealed absorbance changes similar to those of Figure 5I, with no long-lived (10^{-1} s) increase in absorption in the 520–600-nm range. We therefore conclude that the absorbance increase shown in Figure 5IIIc is characteristic of the naphthone analogue and is specific to 337.1-nm excitation. In keeping with its spectral similarity to the phototransients identified as the triplet states of the model compounds XIV and XV, we attribute the increase in absorbance to the triplet state of the bacteriorhodopsin pigment.

To obtain the net contribution of the triplet to the transient difference spectrum, it is necessary to subtract the contribution of the absorbance changes, due to the photocycle, induced by direct excitation of the polyene. This could be carried out due to the fact that, as shown in Figure 5IIc, no absorbance changes above 560 nm are observed later than ~4 ms, after direct (496-nm) excitation of the polyene of bR(XII). Thus, the absorbance changes in Figure 5IIIc, at $\lambda > 560$ nm, are due exclusively to the triplet state, generated by 337-nm excitation of the naphthone moiety. To obtain the triplet-state spectrum at $\lambda < 560$ nm, where the contribution of direct excitation of the polyene is not negligible, we have subtracted the latter by evaluating it according to the following procedure: Subtraction of trace IIIc from IIIa, at $\lambda > 560$ nm, yields the net contribution of the direct-excitation photocycle after 2 μs

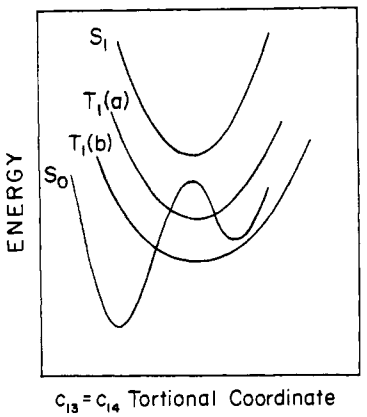

FIGURE 6: Plausible potential energy surfaces including the lowest triplet state of a rhodopsin. In bR the S_0 minimum on the left represents the trans configuration of C_{13}=C_{14}, while that on the right represents the cis configuration characteristic of K (and presumably PK). In the first triplet alternative, T_1(a), the triplet lies above the primary photoproduct (K in bR or bathorhodopsin in visual rhodopsins). In such a case, it may provide a route for thermal noise (thermal forward isomerization) or for back reactions in the photocycles. Both roles are ruled out if the triplet lies below the level of the photoproduct T_1(b). The assumption of a barrierless T_1 surface is arbitrary.

in this wavelength range. Assuming that this is identical with Figure 5IIa, one may use the latter (after appropriate normalization), along with Figure 5IIc, to estimate the contribution of direct-excitation to Figure 5IIIc at $\lambda < 560$ nm. The result, presented as the dotted line in Figure 5III, indicates that the maximum in the triplet difference spectrum is approximately at 540 nm.

Conclusions

Though preliminary in nature, our present results with $RSBH^+$ and with (artificial) bacteriorhodopsin open the way to the investigation of the respective triplet states by intramolecular energy transfer. In the case of bR, introduction of the bulky nonconjugated donor chromophore introduces steric effects that affect the absorption spectrum of the pigment as well as its photocycle and light adaptation process. It cannot be excluded that, at least partially, these effects may be due to perturbations of the protein structure induced by the bulky naphthone substituent. This limitation should be taken into account when applying the present data to the native bR system. We note, however, that although affecting the later stages in the photocycle, it appears that the primary event in the artificial bR, generating a K-like red-shifted intermediate, is analogous to that of the native pigment.

The main straightforward conclusion, derivable from attributing the long-lived 540-nm absorption increase in Figure 5IIIc to the thermalized triplet state of the polyene, is that the latter cannot be an intermediate in the pigment's photocycle. Thus, the $\sim 10^{-1}$ s lifetime of the triplet state is orders of magnitude longer than the ultrafast generation of K. However, an independent question is whether the above triplet state, populated by energy transfer, may initiate the photocycle of bR. This could take place if at least part of the triplet states decay into the (isomerized) PK species. Such a decay mode, which is feasible if the triplet state lies above the PK state (see Figure 6), is difficult to detect on the basis of our present data, due to the fact that both the decay rate and magnitude of the absorbance changes attributed to the observed (long-lived) triplet state are close to those of the last stage of the photocycle of the polyene. Still another possibility is that the triplet state is characterized by more than a single conformation. Thus, a double-well T_1 surface may trap molecules in a 13-cis T_1 minimum that will lead to the fast population of PK, while trans T_1 will lead to the slow, 0.1 s, regeneration of P. As discussed above, this mechanism is not required to account for the generation of PK. The latter can be readily accounted for by that fraction of the 337-nm light that is directly absorbed by the polyene. Further work relevant to this problem will be aimed at designing a triplet-energy moiety with a higher extinction coefficient (with respect to that of the retinyl polyene) so as to reduce the overlapping contributions of the direct-excitation photocycle. Use will also be made of environmental effects (e.g., temperature, solvent composition, degree of hydration, etc.) that will affect the relative decay rates of the triplet state and of the photocycle. An additional goal, aiming at improving our present picture in relation to the triplet state, will be that of designing a bichromophoric retinyl residue with a triplet-energy donor that will not seriously perturb the absorption and the photocycle of the native pigment. This may be achieved by attaching less bulky donors, e.g., benzoquinones, and/or anchoring the donor to a retinal region that is less sensitive to steric interactions with its protein environment.

Assuming that the triplet state is characterized by barrierless potential curves such as those (arbitrarily) drawn in Figure 6, the above information will bear on the possible role of the triplet state in providing a route for back reactions in the photocycle of native and artificial bR, as well as in visual rhodopsins [see Figure 6 and the discussion by Friedman et al. (1989)]. Another problem to which the triplet state may be relevant is the origin of the thermal noise in photoreceptors [see the review by Birge (1989)]. A plausible mechanism for the thermal noise is spontaneous (thermal) isomerization of the C_{11}=C_{12} bond, leading to bathorhodopsin without requiring electronic excitation. As shown in Figure 6, one can envisage a triplet surface [i.e., T_1(a)] that will provide a low activation barrier route to bathorhodopsin via S_0 (rhodopsin, 11-cis, left side, low-energy minimum) → T_1(a) → (bathorhodopsin, all-trans, right side, high-energy minimum).

Registry No. I, 133372-82-4; II (R = H), 133372-83-5; II (R = CH_2CH_2OH), 133323-97-4; III, 133323-83-8; IV, 133323-84-9; V, 133323-85-0; VI, 133323-86-1; VII, 133323-87-2; VIII, 133323-88-3; IX, 133323-89-4; X, 133323-90-7; XI, 133323-91-8; XII, 133323-92-9; XIII, 93-08-3; XIV, 28448-65-9; XV, 133323-94-1; XVI, 133323-96-3; 4-DMAP, 1122-58-3; $BrCH_2CH_2C(OCH_2)_2$, 18742-02-4; Ph_3P=$CHCO_2Et$, 1099-45-2; Me_3CSiMe_2Cl, 18162-48-6; $(EtO)_2P(O)$-$CH_2C(CH_3)$=CHCN, 133323-98-5; $BuNH_2$, 109-73-9; 2-naphthaldehyde, 66-99-9; retinal, 116-31-4; pyrrolidine perchlorate, 22401-44-1.

References

Baasov, T., Friedman, N., & Sheves, M. (1987) *Biochemistry 26*, 3210–3217.

Becker, R. S. (1988) *Photochem. Photobiol. 49*, 369–399.

Becker, R. S., & Freedman, K. (1985) *J. Am. Chem. Soc. 107*, 1477–1485.

Becker, R. S., Freedman, K., Hutchinson, J. A., & Noe, L. J. (1985) *J. Am. Chem. Soc. 107*, 3942–3944.

Birge, R. R. (1981) *Annu. Rev. Biophys. Bioeng. 10*, 315–354.

Birge, R. R. (1989) *Biochim. Biophys. Acta 106*, 293–327.

Closs, G. L., Piotrowiak, P., & Miller, J. (1989) in *Photochemical Energy Conversion* (Norris, J. R., Jr., & Meisel, D., Eds.) pp 23–31, Elsevier Science Publishing Co. Inc., New York.

Fisher, M. M., & Weiss, K. (1974) *Photochem. Photobiol. 20*, 423–432.

Freedman, K., & Becker, R. S. (1986) *J. Am. Chem. Soc. 108*, 1245–1251.

Friedman, N., Sheves, M., & Ottolenghi, M. (1989) *J. Am. Chem. Soc. 111*, 3203-3211.
Harbison, G. S., Smith, S., Pardoen, J., Winkel, C., Lugtenburg, J., Herzfeld, J., Mathies, R., & Griffin, R. (1984) *Proc. Natl. Acad. Sci. U.S.A. 81*, 1706-1710.
Kalisky, O., Goldschmidt, C. R., & Ottolenghi, M. (1977) *Biophys. J. 19*, 185-188.
Nakanishi, R., Balogh-Nair, V., Arnaboldi, M., Tsujimoto, M., & Honig, B. (1980) *J. Am. Chem. Soc. 102*, 7945-7947.
Ottolenghi, M. (1980) *Photochemistry 12*, 97-200.
Ottolenghi, M., & Sheves, M. (1989) *J. Membr. Biol. 112*, 192-212.
Packer, L., Ed. (1982) *Visual Pigments and Purple Membranes. Methods in Enzymology. Biomembranes*, Vol. 88, Part I, Academic Press, New York.
Roush, W., Gillis, H., & Ko, A. (1982) *J. Am. Chem. Soc. 194*, 2269-2283.
Sheves, M., Baasov, T., Friedman, N., Ottolenghi, M., Feinmann-Weinberg, R., Rosenbach, V., & Ehrenberg, B. (1984) *J. Am. Chem. Soc. 106*, 2435-2437.
Smith, S., Myers, A., Pardoen, J., Winkel, C., Mulder, P., Lugtenburg, J., & Mathies, R. (1984) *Proc. Natl. Acad. Sci. U.S.A. 8*, 2055-2060.
Tierno, M., Mead, D., Asato, A., Liu, R., Sekiya, N., Yoshihara, K., Chang, C., Nakanishi, K., Govindjee, R., & Ebrey, T. (1990) *Biochemistry 29*, 5948-5953.
Tokunaga, F., & Ebrey, T. (1978) *Biochemistry 17*, 1915-1922.

Molecular Cloning and Primary Structure of Rat Thyroxine-Binding Globulin[†,‡]

Shuji Imamura,[§] Yuichi Mori,[*,§] Yoshiharu Murata,[∥] Ikuo Yamamori,[§] Yoshitaka Miura,[§] Yutaka Oiso,[§] Hisao Seo,[∥] Nobuo Matsui,[∥] and Samuel Refetoff[⊥]

The First Department of Internal Medicine, Nagoya University School of Medicine, 65 Tsurumai-cho, Showa-ku, Nagoya, 466 Japan, Department of Endocrinology and Metabolism, the Research Institute of Environmental Medicine, Nagoya University, Furo-cho, Chikusa-ku, Nagoya, 464-01 Japan, and Departments of Medicine and Pediatrics, University of Chicago, Chicago, Illinois 60637

Received December 18, 1990; Revised Manuscript Received March 13, 1991

ABSTRACT: Rat thyroxine-binding globulin (TBG) cDNAs were isolated from a rat liver cDNA library by using a human TBG cDNA as a probe. From two overlapping cDNA inserts, an aligned cDNA sequence of 1714 nucleotides was obtained. There was 70% homology with human TBG cDNA over the span of 1526 nucleotides. In order to confirm that the cloned cDNA encodes rat TBG and to localize the NH_2-terminal amino acid of the mature molecule, the protein was purified by affinity chromatography and subjected to direct protein microsequencing. The NH_2-terminal amino acid sequence was identical with that deduced from the nucleotide sequence. The rat TBG cDNA sequenced consisted of a truncated leader sequence (35 nucleotides), the complete sequence encoding the mature protein (1194 nucleotides) and the 3'-untranslated region (485 nucleotides), containing two polyadenylation signals. It was deduced that rat TBG consists of 398 amino acids (M_r = 44 607), three NH_2-terminal residues more than human TBG, with which it shares 76% homology in primary structure. Of the six potential N-glycosylation sites, four are located in conserved positions compared to human TBG. Northern blot analysis of rat liver revealed an approximately 1.8-kilobase TBG mRNA. Its amount increased markedly following thyroidectomy and decreased with thyroxine treatment in a dose-dependent manner.

In many vertebrate species, thyroxine-binding globulin (TBG)[1] serves as a thyroid hormone transport protein in serum (Refetoff et al., 1970). In humans, it is a 54-kDa glycoprotein synthesized in the liver (Murata et al., 1985). Cloning and sequencing of human TBG cDNA revealed homology to another serum transport protein [cortisol-binding globulin (Hammond et al., 1987)] and to serine protease inhibitors (Flink et al., 1986).

The presence of TBG in rat serum was first demonstrated by polyacrylamide gel electrophoresis (Davis et al., 1970). Although similarities between rat and human TBG have been demonstrated in terms of electrophoretic mobility (Davis et al., 1970), structural microheterogeneity (Vranckx et al., 1986), and properties of binding to thyroxine and its analogues (Davis et al., 1970; Sutherland & Brandon, 1976), no direct or deduced information on rat TBG amino acid sequence has been available to explain its distinct immunological properties (Ain et al., 1987; Vranckx et al., 1990a).

Recent work has shown that the very low concentration of TBG in adult rat serum increases remarkably following thyroidectomy (Nanno et al., 1986; Young et al., 1988). This

[†] This work was supported in part by U.S. Public Health Service Grant DK 15070.
[‡] The nucleotide sequence in this paper has been submitted to GenBank under Accession Number J05329.
[*] Address correspondence to this author.
[§] The First Department of Internal Medicine, Nagoya University School of Medicine.
[∥] Department of Endocrinology and Metabolism, the Research Institute of Environmental Medicine, Nagoya University.
[⊥] Departments of Medicine and Pediatrics, University of Chicago.

[1] Abbreviations: TBG, thyroxine-binding globulin; M_r, molecular weight; 2DGE, two-dimensional gel electrophoresis; PVDF, poly(vinylidene difluoride).

0006-2960/91/0430-5406$02.50/0